MODIFIED EVERITT-JENNINGS: A COMPLETE METHODOLOGY FOR PRODUCTION OPTIMIZATION OF SUCKER ROD PUMPED WELLS

Victoria Pons
Weatherford

ABSTRACT

When using artificial lift, namely sucker rod pumps, there are three major factors to consider when trying to control and optimize production: elasticity, viscous friction and mechanical friction. The Modified Everitt-Jennings uses an iteration on dual damping factors to approximate the correct amount of viscous friction to be removed to mimic the energy lost through the viscous forces imparted on the outer diameter of the rods by the fluids.

A precise Fluid Load Line Calculation provides a concavity test to diagnose the presence of mechanical friction. Secondly, in order to maximize production and prevent rod string damage, pump-off control technology must be used in conjunction with sucker rod pump installation. The most accurate type of pump-off control is one using pump fillage. The Modified Everitt-Jennings combines an in-depth stress analysis with a powerful Pump Fillage Calculation, which outputs correct pump fillage regardless of downhole conditions present.

In this paper, a complete methodology for controlling sucker rod pumps is presented. This methodology combines state of the art, innovative methods that smartly and efficiently automate the control of sucker rod pumped wells.

INTRODUCTION

Reciprocating Rod Lift represents over 85% of the world's artificial lift. Sucker rod pumping wells can be analyzed with surface dynamometer systems or more accurately with a downhole dynamometer. Unfortunately, downhole dynamometers are an expensive and impractical commodity. Therefore, it is common practice to calculate downhole data from measured surface data.

When using reciprocating rod lift, there exists three major factors impeding the motion and efficiency of the system: elasticity, viscous friction and mechanical friction.

Because of the cyclic loading and unloading, stress waves travel up and down the rod string at the speed of sound. Secondly the viscous fluids impart a viscous force on the outer diameter of the rod string opposing the motion of the rods. Finally, mechanical friction occurs when the rod string or couplings get into contact with the tubing.

In the case of a vertical-hole model, where mechanical friction is small enough that it can be neglected, the rod string can be compared to an ideal slender bar. Therefore the propagation of stress waves becomes a 1-D phenomenon. The 1-D damped wave equation models the propagation of stress waves down an ideal slender bar, see [13]. The one-dimensional damped wave equation is most commonly used to model the behavior of the stress waves traveling down the rod string.

Other methods for solving the wave equation include the method of characteristics by Snyder, see [12], separation of variables and Fourier series by Gibbs, see [4,6], and finite differences by Knapp, see [7]. In 1976, Everitt and Jennings applied finite differences to the wave equation and outlined an algorithm for iterating on the net stroke and damping factor, see [3, 11]. The Everitt-Jennings method has been implemented and modified by Weatherford, in [2]. The Everitt-Jennings method was enhanced by the addition of a pump fillage calculation capable of calculating pump fillage regardless of downhole conditions. Also, the original iteration on the net stroke and damping proposed by Everitt and Jennings in [3, 11] has been modified and improved by adding a concavity test and allowing for an iteration on single or dual damping factors.

In this paper, a synthesis of the Modified Everitt-Jennings (MEJ) package is presented. This includes iteration on damping, Pump Fillage Calculation (PFC), Fluid Load Line Calculation (FLLC) as well as stress analysis.

In Section 2, the MEJ and above-mentioned methods are presented.

In Section 3, results from the application of MEJ to field data are presented. Also in this section, results showing the effectiveness of the pump fillage calculation are presented.

Conclusions follow in Section 4, while figures are presented at the end of the paper.

2. MATERIAL AND METHODS

In this section, the modified Everitt-Jennings method is described in the first subsection. In the next subsection, the iteration on damping, the Fluid Load Line Calculation, the Pump Fillage Calculation as well as the stress are detailed.

2.1. The modified Everitt-Jennings method.

The key to being able to diagnose and control a rod-pumped well is the ability to simulate exactly the behavior of the rod string downhole. However, due to the sucker rod string's elasticity, it is difficult to calculate downhole data from measured surface data.

The elastic force acting on the sucker rod string takes the form of stress waves traveling down the sucker rod string at the speed of sound. As such, the sucker rod string being physically equivalent to an ideal slender bar renders the propagation of stress waves a one-dimensional phenomenon.

Downhole conditions can be correctly calculated from the surface data using the one-dimensional damped wave equation. Let $u = u(x,t)$ be the displacement of position x at time t.
The condensed one-dimensional wave equation reads:

$$v^2 \frac{\partial^2 u}{\partial x^2} = \frac{\partial^2 u}{\partial t^2} + c\frac{\partial u}{\partial t}, \tag{1}$$

where the acoustic velocity is given by: $v = \sqrt{\frac{144Eg}{\rho}}$.

It is important to note that the friction referred to in the previous equation corresponds to viscous friction. The friction present in a well is a combination of two forces: the viscous friction force and the Coulombs friction force.

The above equation describes the propagation of stress waves in a vertical hole model or near vertical model. In this case the Coulombs friction or mechanical friction is negligible. Coulombs friction arises when there is contact between the tubing, the rods and the rod couplings. This most often happens when dealing with horizontal wells. The above equation is not suitable for horizontal wells since it only takes into consideration longitudinal movement of the rods and not lateral movement. For more details on the treatment of deviated wells, see [5, 8, 10].

Let A be the sucker rod string's cross sectional area (in.^{2}), ρ the sucker rod string's density (lbm/ft^3), k the friction coefficient and E the modulus of elasticity (psi). The gravity constant is given by g (32.2 (lbm-ft)/(lbf-sec^2)). In order to account for varying rod diameters, (1) can be expanded as follows:

$$EA\frac{\partial^2 u}{\partial x^2}(x,t) = \frac{\rho A}{144g}\frac{\partial^2 u}{\partial t^2}(x,t) - c\frac{\rho A}{144g}\frac{\partial u}{\partial t}(x,t), \tag{2}$$

where c is the damping factor. The wave equation is derived in detail in [13].

The one-dimensional wave equation was originally solved and made commercially available in 1967 by Gibbs, in [6], using separation of variables and truncated Fourier series. In order to solve this linear hyperbolic differential equation, Everitt and Jennings in [3] used a finite difference model.

First-order-correct forward differences and second-order-correct central differences are used as analogs for the first derivative and second derivative with respect to time respectively. A slightly rearranged second-order-correct central difference is used as the analog for the second derivative with respect to position, to accommodate for different taper properties.

The boundary conditions for the above equation are obtained directly from the surface position versus time and load versus time data. The desired solutions, being only the periodic solutions, (2) do not require initial conditions, see [3]. Let N be the number of recorded surface data points and M be the total number of finite difference nodes along the rod string down the wellbore, such that M is the last point above the pump. Let $\{i\}_1^M$ represent the vector of finite difference nodes along the rod string. Let $\{j\}_1^N$ represent the vector of sample points taken at the surface. Let $\{g_{PR}\}_1^N$ and $\{f_{PR}\}_1^N$ be the discrete functions comprised of the surface polished rod position versus time and surface polished rod load versus time data respectively.

The finite difference analogs are replaced in (2) to give:

- Initialization: For $j = 1, \cdots, N: \ u_{0,j} = \ g_{PR,j}$.

- From Hooke's law: For $j = 1, \cdots, N: \ u_{1,j} = \frac{f_{PR,j} \cdot \Delta x}{EA} + u_{0,j}$.

- For $i = 2, \cdots, M$:

$$u_{i+1,j} = \frac{1}{\left(\frac{EA}{\Delta x}\right)^+} \left\{ [\alpha(1 + c\Delta t)] \cdot u_{i,j+1} - \left[\alpha(2 + c\Delta t) - \left(\frac{EA}{\Delta x}\right)^+ - \left(\frac{EA}{\Delta x}\right)^- \right] \cdot u_{i,j} + \alpha \cdot u_{i,j-1} - \left(\frac{EA}{\Delta x}\right)^- \cdot u_{i-1,j} \right\}, \tag{3}$$

where $\alpha = \frac{\overline{\Delta x}}{\Delta t^2} \left[\frac{\left(\frac{\rho A}{144g}\right)^+ + \left(\frac{\rho A}{144g}\right)^-}{2} \right]$ and $\overline{\Delta x} = \frac{1}{2}(\Delta x^+ + \Delta x^-)$.

- At the pump:

$$u_{pump,j} = (1 + c\Delta t) \cdot u_{M-1,j+1} - c\Delta t \cdot u_{M-1,j} + u_{M-1,j-1} - u_{M-1,j},$$
$$F_{pump,j} = \frac{EA}{2\Delta x} \left(3u_{M,j} - 4u_{M-1,j} + u_{M-2,j} \right).$$

In the previous algorithm, c is the damping factor.

Everitt and Jennings devised a method for iterating on the net stroke and damping factor in [3]. The rod string is, therefore, split into M finite difference nodes of length L_i (ft), density ρ_i (lbm/ft^3) and area A_i (in^2). The damping factor is given by:

$$c = \frac{(550)(144g)}{\sqrt{2}\pi} \frac{(H_{PR} - H_H)\tau^2}{(\sum \rho_i A_i L_i) S^2}, \tag{4}$$

Where H_{PR} is the polished rod horsepower (hp), S is the net stroke, τ is the period of one stroke (sec.) and H_{hyd} is the hydraulic horsepower (hp) obtained as follows:

$$H_{hyd} = (7.36 \cdot 10^{-6}) Q \gamma F_l, \tag{5}$$

where Q is the pump production rate (B/D), γ is the fluid specific gravity and F_l is the fluid level (ft). For more details on the derivation of (5), see [3].
The calculation of the hydraulic horsepower requires knowing the fluid level and the pump production rate. The pump production rate is computed with:

$$Q = (0.1166)(SPM) S \, D^2, \tag{6}$$

where SPM is the pumping unit speed (SPM), D is the pump diameter (in^2).

The MEJ automatically selects a number of finite difference nodes that will not only satisfy the stability condition but also homogenize the spacing of said finite difference nodes throughout the rod string. This enables the output of load and stress at any finite difference node down the wellbore. The code is written in such a way as to automatically compute a range of numbers of finite difference nodes satisfying the stability condition, see [2].

2.2. The Iteration on dual damping.

In this subsection the iteration on the net stroke and damping is examined.

The above equations are for the most part straight forward. However it is important to note that the fluid level and the net stroke are not known at the beginning of the calculation. The fluid level reflects the amount of fluid present in the wellbore annulus and may constantly change during the pumping cycle of a well. The fluid level, unless shot for that particular stroke, might not reflect current downhole conditions.

The great advantage of the automatic iteration on the net stroke and the damping factor is the fact that the damping factor is adjusted automatically without human intervention. Users, when managing a medium to large group of wells, do not have to spend time manually adjusting the damping factor as may be required by other methods.

Everitt and Jennings proposed an algorithm for the iteration on the net stroke and damping factor, which and can be found in [3]. In the original algorithm, Everitt and Jennings use the pump and hydraulic horsepower as convergence criteria for the iteration on damping. This idea is conserved and enhanced with a concavity testing, which is an integral part of the Fluid Load Line Calculation (FLLC). The original iteration on the net stroke and damping factor was modified in order to provide more accurate results in the field.

The original iteration on damping proposed by Everitt and Jennings in [3] was originally modified to be more reliable in field testing. An initialization step was added to speed up convergence and make the initial variables more accurate. In a second step, the iteration on damping was split into a separate iteration on the upstroke and the downstroke.

An initial computation of the downhole data using a fixed damping factor is conducted first in order to start with more accurate values for the fluid level, net stroke and production rate. Due to the fact that the net stroke varies only little with the variation of the damping factors, the iteration on the net stroke is done first. Once the iteration on the net stroke is done, the iteration on the damping factor begins. The iteration on the damping factor consists in comparing the values for the hydraulic horsepower and the pump horsepower. Ideally these two quantities should be equal. If the hydraulic horsepower and the pump horsepower are not equal, the algorithms enter a damping variation algorithm based on results from the FLLC.

Flowcharts for the iteration on single damping and dual damping are given in Figures 1-4.

The damping variation algorithm is necessary since even though this model is a vertical-hole model, often it is used on wells with significant deviation. In that case the presence of mechanical friction can make the convergence of those two quantities very difficult.

When using dual damping factors, the convergence criteria can be more precise and the upstroke can converge independently of the downstroke and vice versa.

2.2.2. Splitting the damping factor into upstroke and downstroke damping.

Realistically, the upstroke and downstroke damping can be very different. On the downstroke the rods moves against the fluids, while on the upstroke the rods moves with the fluids. Therefore, it is necessary to account for that difference by allocating a separate damping factor for the upstroke and for the downstroke.

For each stroke, the top of stroke is calculated. The top of stroke is the turning point at which the upward movement of the pumping unit stops and the downstroke motion begins, making it the delimiting factor between the downstroke and upstroke. The top of stroke is computed by calculating the zero of the first derivative of the position $u = u(x,t)$, i.e. the velocity. For more details on that computation, see [1].

The modified Everitt-Jennings finite difference algorithm, including the changes associated with treating two damping factors, reads as follows:

- Initialization: For $j = 1, \cdots, N: \; u_{0,j} = g_{PR,j}$.
- From Hooke's law: For $j = 1, \cdots, N: \; u_{1,j} = \frac{f_{PR,j} \cdot \Delta x}{EA} + u_{0,j}$.
- For $i = 2, \cdots, M$:

  For $j = 1, \dots, TOS$:

$$u_{i+1,j} = \frac{1}{\left(\frac{EA}{\Delta x}\right)^{+}} \left\{ \left[\alpha\left(1 + D_{up}\Delta t\right)\right] \cdot u_{i,j+1} - \left[\alpha\left(2 + D_{up}\Delta t\right) - \left(\frac{EA}{\Delta x}\right)^{+} - \left(\frac{EA}{\Delta x}\right)^{-}\right] \cdot u_{i,j} + \alpha \cdot u_{i,j-1} - \left(\frac{EA}{\Delta x}\right)^{-} \cdot u_{i-1,j} \right\}, \tag{7}$$

  For $j = TOS + 1, \dots, N$:

$$u_{i+1,j} = \frac{1}{\left(\frac{EA}{\Delta x}\right)^{+}} \left\{ \left[\alpha(1 + D_{down}\Delta t)\right] \cdot u_{i,j+1} - \left[\alpha(2 + D_{down}\Delta t) - \left(\frac{EA}{\Delta x}\right)^{+} - \left(\frac{EA}{\Delta x}\right)^{-}\right] \cdot u_{i,j} + \alpha \cdot u_{i,j-1} - \left(\frac{EA}{\Delta x}\right)^{-} \cdot u_{i-1,j} \right\}, \tag{8}$$

where $\alpha = \frac{\overline{\Delta x}}{\Delta t^2}\left[\frac{\left(\frac{\rho A}{144g}\right)^{+} + \left(\frac{\rho A}{144g}\right)^{-}}{2}\right]$ and $\overline{\Delta x} = \frac{1}{2}(\Delta x^{+} + \Delta x^{-})$.

- At the pump:

  For $j = 1, \dots, TOS$:

$$u_{pump,j} = \left(1 + D_{up}\Delta t\right) \cdot u_{M-1,j+1} - D_{up}\Delta t \cdot u_{M-1,j} + u_{M-1,j-1} - u_{M-1,j}, \tag{9}$$

  For $j = TOS + 1, \dots, N$:

$$u_{pump,j} = (1 + D_{down}\Delta t) \cdot u_{M-1,j+1} - D_{down}\Delta t \cdot u_{M-1,j} + u_{M-1,j-1} - u_{M-1,j}, \tag{10}$$

  For $j = 1, \dots, N$:

$$F_{pump,j} = \frac{EA}{2\Delta x}\left(3u_{M,j} - 4u_{M-1,j} + u_{M-2,j}\right).$$

In equation (7-10), the upstroke damping factor D_{up} is used for $j = 1, \dots, TOS$ while the downstroke damping factor D_{down} is used for $j = TOS + 1, \dots, N$.

In the next sub section, the damping variations for the iteration on dual damping factor are detailed.

2.2.3. Description of the algorithm for the iteration on dual damping factors.

The iteration on the net stroke and the iteration on the damping factor(s) read as follows:

1) Guess net stroke (NS_0)
   Guess top of stroke (TOS)
   Compute daily production rate (Q)
   Compute hydraulic horsepower (H_{hyd})
   Set damping factors. $D_{up} = 0.25$, $D_{down} = 0.5$.

2) Compute downhole data
Get top of stroke (TOS)
Compute actual fluid load lines ($F0_{up}$actual, $F0_{down}$actual)
Calculate net stroke (NS)
Calculate fluid level (Fl)
Calculate damping factors ($D_{up,}$ D_{down})

3) Is the absolute value of the difference between the guess net stroke and the calculated net stroke within tolerance? If yes, proceed to dual iteration on the damping Step 6. If no, continue iterating on the net stroke and proceed to Step 4.

4) Calculate daily production rate (Q)
Calculate hydraulic horsepower (H_{hyd})
Calculate damping factors (D_{up}, D_{down})
Compute downhole data

5) Is the absolute value of the difference between the previous net stroke and new net stroke within tolerance? If yes, proceed to dual iteration on the damping Step 6. If no, continue iterating on the net stroke and go back to Step 4.

6) Calculate daily production rate (Q)
Calculate hydraulic horsepower (H_{hyd})
Calculate damping factors (D_{up}, D_{down})

7) Compute downhole data
Compute calculated fluid load lines ($F0_{up}$calc, $F0_{down}$calc)
Compute pump horsepower (H_{pump})

8) Enter Damping Variation Algorithm. If successful exit, else go back to Step 7.

The above algorithm is given in the form of a flowchart in Figure 1 and 2.

The values for the calculated and actual fluid load lines are compared to determine if the upstroke and downstroke damping factors should be updated. This process serves as a test of concavity of sorts, as mentioned above.

In the damping variation algorithm, the direction of the variation on the damping factors is determined by the sign of the difference between the pump horsepower and the hydraulic horsepower. If the pump horsepower is greater than the hydraulic horsepower, the data is deemed to not have enough damping. Consequently, the damping factors need to be increased. Similarly, if the pump horsepower is less than the hydraulic horsepower, the data is deemed to have too much damping and the damping factors need to be decreased. However, another test is set in place to determine if the damping factors should be increased.

In the case of the dual damping factors, the convergence criteria for upstroke can be treated separately from the convergence criteria for the downstroke. Only the damping variation algorithm for the iteration on dual damping is given below.

The algorithm to determine the change in the damping factors is as follows:
1) Is the pump horsepower H_{pump} within tolerance of the hydraulic horsepower H_{hyd}? If yes, the iteration is successful and exits. If no, go to Step 2.

2) Is the calculated upstroke fluid load within range of the actual upstroke fluid load? And, is the calculated downstroke fluid load within range of the actual downstroke fluid load? If yes, the iteration is successful and exits. If no, go to Step 3 or Step 4.

3) Is the pump horsepower greater than the hydraulic horsepower? If yes,

a) Is the calculated upstroke fluid load greater than the actual upstroke fluid load? If yes, update upstroke damping factor. If no, no update is necessary.
b) Is the calculated downstroke fluid load less than the actual downstroke fluid load? If yes, update downstroke damping factor. If no, no update is necessary.

4) Is the pump horsepower less than the hydraulic horsepower? If yes,
a) Is the calculated upstroke fluid load less than the actual upstroke fluid load? If yes, update upstroke damping factor. If no, no update is necessary.
b) Is the calculated downstroke fluid load greater than the calculated downstroke fluid load? If yes, update downstroke damping factor. If no, no update is necessary.

More on this algorithm can be found in [9].

In the next sub-subsection, the computation of the fluid load lines and the concavity testing are presented.

2.3. Fluid Load Line Calculation (FLLC) and Concavity Testing.

Ideally, the graphical representation of the upstroke and the downstroke should be horizontal lines. If the downhole card is concave, too much damping is used when solving the one-dimensional damped wave equation. Similarly, if the downhole card is convex, too little damping is used when solving the one-dimensional damped wave equation.

In the event that the pump horsepower and the hydraulic horsepower are not within tolerance and the damping needs to be adjusted, a second set of tests takes place. This test compares the statistical distributions of the upstroke points and the downstroke points to the computed values of the fluid load lines. Essentially, the concavity of the upstroke and downstroke lines is tested.

The fluid load lines are determined by using the first and second derivatives of the position. The upstroke fluid load line referred in this paper as $F0_{up}$ while the downstroke fluid load line is referred to as $F0_{down}$.
The actual fluid load lines $F0_{up}actual$ and $F0_{down}actual$ are computed using the first and second derivatives of the downhole data. The upstroke actual fluid load line $F0_{up}actual$ is calculated as the load corresponding to the top of stroke. The top of stroke is computed by finding the zero of the first derivative of the downhole position data. In order to compute the downstroke actual fluid load line $F0_{down}actual$, the location of the transfer point must be calculated. The transfer point is the point at which the load is transferred from the traveling valve to the standing valve. The transfer point is computed using a pump fillage calculation, see [1]. The actual fluid load line $F0_{down}actual$ is taken to be the load of the absolute minimum of the second derivative of the downhole position data after the transfer point, i.e. the lower right corner of the downhole card.

The upstroke and downstroke data is statistically ordered by load in order to produce a probability density function. The maximums of the probability functions yield a set of load ranges in which most of the upstroke and downstroke data reside. The maximum of the probability density function for the upstroke data is referred to as the calculated fluid load line $F0_{up}calc$ while the maximum of the probability density function for the downstroke data is referred to as the calculated fluid load line $F0_{down}calc$.

The concavity test mentioned above can also be used to detect the presence of mechanical friction, at which point the iteration on damping is stopped as to not falsify the data and the rest of the methods switch control to adapt to the presence of mechanical friction.

In the next sub-sub-section, the separation of the damping into an upstroke damping factor and a downstroke damping factor, for the iteration on dual damping factors, is presented.

In the next sub-section, the pump fillage calculation is detailed.

2.4. The pump fillage calculation.

In this subsection the pump fillage calculation algorithm is detailed.

The algorithm mentioned above is composed of three methods and determines the transfer point and therefore the pump fillage of a given pump stroke. The results from these three methods are then “checked” by a fourth method, which guarantees that a correct pump fillage values is achieved at each pump stroke for a given well.
The methods described below are based on finding the transfer point, i.e. the point in the stroke at which the fluid column is transferred from the standing valve to the traveling valve. Looking at the graphical representation of a downhole card this point is defined as the point after the top of stroke when the loads decrease dramatically.
A flowchart of the algorithm is shown in Figure 3.

2.4.1. The method of Positions

The first method relies solely on the downhole position versus time data. It can be observed that the graph of the downhole position versus time data resembles an ideal sinusoidal curve, when the well is full. However when the fluids in the reservoir are low and fluid pound begins, the distribution of the downhole position versus time data still has a sinusoidal curve shape but displays a plateau after the top of stoke. This plateau corresponds to the plunger moving down but not yet hitting fluid.

The first method uses calculus in an effort to locate the change in concavity created by the plateau. At the top of stroke, the graph is concave down. At the plateau the graph changes to concave up and then back to concave down after the plateau. This first change in concavity is the phenomenon the first method is trying to isolate. Let $f(x)$ be a function and let $f''(x)$ be its second derivative. Then the graph of $f(x)$ is concave down if and only if $f''(x) < 0$, and concave up if and only if $f''(x) > 0$. The change in concavity is characterized by $f''(x) = 0$.

First, the top of stroke is located. The top of stroke is the point at which position values move from increasing to decreasing. In other words, the top of stroke corresponds in most cases to the critical point of the downhole position versus time data. In order to compute the critical point of a function, the first derivative of the downhole position, $p'(t)$, must be approximated and then set to zero. When dealing with a discrete function, the first derivative can be understood to be the difference between two consecutive values of the function. Since the surface position versus time function and load versus time functions are taken at regularly timed spaced intervals, without loss of generality, the downhole data can also be assumed to be equally spaced. The first and second derivatives are taken to be the difference between two consecutive points of the downhole position data and the first derivative of the downhole position data respectively. The critical point can be obtained by finding where the discrete first derivative function intersects the x-axis.

The local maximum formed by the plateau in the downhole position versus time data, can be identified using the second derivative of the downhole position versus time data. As mentioned above the plateau is characterized by a change in concavity. Therefore it is necessary to find the absolute minimum of the second derivative of the downhole position with respect to time after the critical point or top of stroke.

The transfer point is located by finding the maximum of the second derivative of the downhole position between the top of stroke and the absolute minimum of the same second derivative. Note that the actual location of the transfer point might not be exactly at the maximum of the second derivative between the TOS and the absolute minimum, but through research the maximum has shown to be a very reliable guess.

2.4.2. The method of Loads

The second method relies solely on the downhole load versus time data. As mentioned above, the transfer point is characterized as the point at which the fluid load is transferred from the standing valve to the traveling valve. Graphically this translates into a sudden drop of the loads on the rod string. Therefore locating the transfer point is equivalent to locating the sharp gradient in the downhole load versus time data. The sharp gradient is characterized by the absolute minimum of the first derivative of the downhole load versus time data, i.e. the point at which the downhole load versus time data has the most negative slope or drop.

2.4.3. The method of Ordering

The third method is based on splitting the downhole data into two categories, differentiated by an imaginary half-line. The half-line corresponds to the load span divided by two. The downhole data is then organized into top points and bottom points by taking the top eighth and the bottom eighth of the downhole card. The average top value and bottom value are computed as well as the average middle value corresponding to the point where the imaginary half line crosses the downhole card on the downstroke. The pump fillage is taken to be a combination of the ratios of the position values associated with the average bottom value, the average middle value and the average top value. Depending on the well and reservoir conditions, the distribution of the downhole data differs drastically. For example if the reservoir fluids contain a lot of gas, as the plunger goes down, it encounters gas instead of fluid. The gas within the barrel softens the descent of the plunger.This results in a downhole position versus time data which does not display a plateau and resembles a perfect sinusoidal curve elongated on one side. Also in the case of a deviated well, the downhole position versus time data might display several plateaus as resulting from the tubing going around the corners.

Because it is obvious that well and reservoir conditions can vary dramatically from well to well and from stroke to stroke, relying solely on one method would lead to error. It is not feasible that one method could accurately determine pump fillage in every condition encountered. However, it is more appropriate to rely on a combination of methods each having different strengths.

2.4.4. The Multiple Pump fillage Method

As mentioned above, since well conditions can vary dramatically, in some cases, the above methods might not all compute an accurate pump fillage. It is therefore essential to be able to determine which method is correct. In an effort to do that, a fourth method was designed to approximate the correct pump fillage range. The idea behind this method is to compute the pump fillage at multiple locations of the downhole card. From this set of pump fillage values, a probability density function is obtained. The probability density function shows the distribution of the pump fillage values.

Let M be the number of locations or segments of the downhole card, at which the pump fillage is computed. The load span of the downhole card is obtained from the maximum and minimum load values of the downhole data. Dividing the load span by M gives us the spacing for each segment. Let $L_{i=1,\cdots,M}$ be the load values for each segment.

The top of stroke, TOS, of the card is calculated, as described in the method of positions.
Let $p(x)$ be the downhole position data. Let $\{t_i\}_{i=1,\cdots,M}$, be the segments of the downhole card. The position at the top of stroke is found by $p(t_{TOS})$. In order to compute the set of pump fillage values, the position $p(t_i)$ is found for each segment, by finding the first position at which the loads crosses the i^{th} load segment L_i . The pump fillage for that segment is calculated as:

$$PF_i = 100 \cdot \frac{p(t_i)}{p(t_{TOS})}.$$

This procedure yields a set of Mpump fillage values per card ranging from 0 to 100. In order to obtain the probability density function, the pump fillage range must be split into I intervals. Let K be the interval spacing. Then let

$$s(j) = 0 + (j-1) \cdot \frac{100}{K}, j = 1, \cdots, K.$$

be the interval indexes. The probability density function $pdf(t)$ is computed by sorting the pump fillage values PF_i , $i = 1, \cdots, M$ into the intervals $[s(j), s(j+1)]$, $j = 1, \cdots, K$, and recording the number of occurrences per interval.

The final pump fillage value output from the pump fillage calculation is the average results of the above three methods which belong to the first interval. In the event that the pump fillage values from the above methods do not belong to the first interval, the pump fillage can be set to either the average of the above pump fillage methods belonging to the second interval or set to the middle of the first interval.

Through research, it can be inferred that in the event when none of the above methods manage to yield a pump fillage belonging to the first interval, setting the pump fillage to the average of the methods belonging to the second interval yields more accurate results.

The intervals with the highest concentration of pump fillage values is called the first interval and is the interval in which the actual pump fillage is most likely to be found. The interval with the second highest concentration of pump fillage values is called the second interval.

For more details on the above algorithm, refer to [1].
In the next sub-section, the stress analysis is presented.

2.5. Stress Analysis

Stress Analysis is the practice of evaluating the stress distribution within a given material.
There are two types of failures when dealing with sucker-rod pumps, tensile failures and fatigue failures.
Tensile failures are rare and occur when the rods are over-stressed, i.e. the force exerted on the material results in an axial pulling force overcoming the tensile strength of the material. For example, excessive pull is applied to the rods, in which case the rod stress can exceed the rod material tensile strength causing a tensile break.

Tensile failures will mainly happen in the rod body, where the cross-sectional area is at a minimum. Tensile failures materialize in a permanent stretch and small breaks in the rod. At that point, if the rods are run again, those points become stress raisers since the load bearing cross-sectional area is reduced.

Rod failures are mostly attributed to fatigue breaks, which occur at stress levels well below the ultimate tensile strength or even below the yield strength of the steel rods. Repeated stresses cause material fatigue or plastic tensile failure. The failure starts at some stress raiser on the surface of the rod. The incurred crack then progresses in a direction perpendicular to the stress across the rod, therefore reducing the cross sectional area capable of carrying the load, at which point the rod breaks.

Using finite differences as a tool to solve the wave equation enables the creation of a mesh, i.e. a space and time discretization, position, load and therefore stress can be computed at any finite difference node.

Rod strings are subject to cyclic loading, which creates a pulsating tension on the rod string. During the upstroke, the rods carry the load of the fluids, the dynamic loads and the friction forces. On the downstroke; the rods carry the weight of the rods without the dynamic loads and friction.

As mentioned above, changes in cross sectional area in the rod string create areas of concentrated local stress.
In an effort to provide a complete and thorough stress analysis, the finite difference elements, or nodes, are selected in such a way that the Δx or spacing in between each node is of similar magnitude for each taper. This process is initiated by first picking an initial number of finite difference nodes (per taper) satisfying the stability condition. The minimum Δx for all tapers is then used to compute the necessary number of finite difference elements for the rest of the tapers to ensure a uniform mesh. The use of a quasi-uniform mesh allows for a more detailed and practical analysis of the stress functions.

The stress data created is a series of values, which are taper specific. The progression of the stress data per taper follows a quasi linear behavior. In other words, the maximum tensile stress occurs at the bottom surface, while the maximum compression stress occurs at the top surface, varying linearly from top to bottom. However in the event that there exists a stress raiser among one section of the rod, the behavior of the stress point ceases to be linear.

A cubic spline interpolation, however, involves only four constants for each stress data point in order to approximate each taper. The advantage of using a cubic spline interpolation is that it is a relatively simple and available method in literature. Also, cubic splines being polynomials of third degree are therefore continuously differentiable on the taper interval, providing a continuous second derivative. Calculus methods can therefore be used on the smooth cubic spline interpolant in order to search for possible stress raisers and imperfections in the stress data, which could in turn imply a future failure.

Using the stress versus depth data, a cubic spline interpolant is generated for each taper.
The tridiagonal system generated during the cubic spline interpolation is solved using Crout Factorization, or similar methods.

The stress analysis table and graph are available to users in LOWIS software.

In the next section, results and discussion are presented.

3. RESULTS AND DISCUSSION

In this section results concerning the accuracy of the modified Everitt-Jennings algorithm enhanced with the pump fillage calculation are presented.

For each of the following results, field data corresponding to different downhole conditions are selected. For each of these wells, the graphical representation of the downhole card is displayed. For each of these examples, results from the PFC, FLLC, iteration on damping as well as stress analysis are displayed.

On the graphical representation of the downhole card, two sets of fluid load lines are displayed. The red fluid load lines represent the theoretical fluid load line or actual fluid load lines. The blue fluid load lines represent the calculated fluid load lines obtained through statistics, depicting the load value at which most of the upstroke and downstroke points lie.

As part of the results, the values of the PFC are also presented. These results include the pump fillage values obtained through each of the methods of Position, Loads and Orders as well as the first and second interval of likelihood. The value for the final pump fillage is also displayed. Additionally the tubing gradient obtained through multiphase flow computation as well as the calculated fluid level are displayed. These values are computed for each stroke.

For the results of the iteration on damping, the values for the polished rod horsepower, pump horsepower and hydraulic horsepower are displayed. The results of the iteration on damping are also presented with the values for the iterated netstroke, upstroke and downstroke damping factors. The number of iterations for the iteration on the netstroke and damping are presented below.

In Figure 4, results from the MEJ package are applied to field data Example 1. The theoretical fluid load lines read 1219 and -193 lbs, while the calculated fluid load lines read 1561 and -546. The polished rod horsepower is 0.87 while the pump horsepower is 0.76.

The upstroke damping factor is 0.25 while the downstroke damping factor is 0.25. The hydraulic horsepower is 1.19, clearly erroneous from wrong input. Since the pump horsepower is smaller than the polished rod horsepower and the F0_up_calc is greater than the F0_up_theo, this indicates the presence of mechanical friction, almost 300 lbs of Coulombs friction. The calculated fluid level is 1160, and the tubing gradient is 0.36. The iteration on netstroke converged in 2 iterations while the interation on damping converged in 1 iteration.

The method of Position calculated 64.51 % pump fillage, while the method of Loads 59.82 and the method of Positions 64.51. The first interval of most likelihood is [61, 64] and the second is [64, 67]. The final pump fillage value is 62.94%.

In Figure 5, results from the MEJ package are applied to field data Example 2. The theoretical fluid load lines read 4876 and -920 lbs, while the calculated fluid load lines read 4818 and -931. The polished rod horsepower is 8.01 while the pump horsepower is 6.84.

The upstroke damping factor is 0.25 while the downstroke damping factor is 0.5. The hydraulic horsepower is 5.58, clearly erroneous from wrong input. For this card the damping iteration stops since the fluid load lines are within tolerance of each other. This well also displays upstroke pump wear. The calculated fluid level is 7285, and the tubing gradient is 0.45. The iteration on netstroke converged in 2 iterations while the interation on damping converged in 1 iteration.

The method of Position calculated 100.00 % pump fillage, while the method of Loads 100.00 and the method of Positions 100.00. The first interval of most likelihood is [100, 101] and the second is [91, 94]. The final pump fillage value is 100.00 %.

In Figure 6, results from the MEJ package are applied to field data Example 3. The theoretical fluid load lines read 4415 and -276 lbs, while the calculated fluid load lines read 4815 and -354. The polished rod horsepower is 2.67 while the pump horsepower is 2.28.

The upstroke damping factor is 0.25 while the downstroke damping factor is 0.5. The hydraulic horsepower is 3.7, clearly erroneous from wrong input. This well is pumped off with upstroke pumpwear. The calculated fluid level is 6558, and the tubing gradient is 0.4. The iteration on netstroke converged in 2 iterations while the interation on damping converged in 1 iteration.
The method of Position calculated 60.70 % pump fillage, while the method of Loads 60.35 and the method of Positions 61.01. The first interval of most likelihood is [61, 64] and the second is [58, 61]. The final pump fillage value is 60.69%.

In Figure 7, results from the MEJ package are applied to field data Example 4. The theoretical fluid load lines read 3172 and -97 lbs, while the calculated fluid load lines read 2967 and -241. The polished rod horsepower is 6.42 while the pump horsepower is 5.29.

The upstroke damping factor is 0.25 while the downstroke damping factor is 0.99. The hydraulic horsepower is 3.08, clearly erroneous from wrong input. This well displays a lot of shock waves traveling through the rod string. Also possibly from improper configuration of material at the well site note that the loads on the left hand side of the card are lower than the loads on the right side, therefore giving the slanting appearance to the card. This can make the computation of fluid load and pump fillage difficult. The calculated fluid level is 2707, and the tubing gradient is 0.39. The iteration on netstroke converged in 2 iterations while the interation on damping converged in 2 iterations. The method of Position calculated 92.05 % pump fillage, while the method of Loads 92.05 and the method of Positions 92.21. The first interval of most likelihood is [91, 94] and the second is [97, 100]. The final pump fillage value is 92.10 %.

In Figure 8, results from the MEJ package are applied to field data Example 5. The theoretical fluid load lines read 1381 and -158 lbs, while the calculated fluid load lines read 1665 and -299. The polished rod horsepower is 1.66 while the pump horsepower is 1.40.

The upstroke damping factor is 0.76 while the downstroke damping factor is 0.99. The hydraulic horsepower is 1.21, clearly erroneous from wrong input. This well is tagging bottom with some mechanical friction, as in the previous case almost 300 lbs of Coulombs friction. The calculated fluid level is 2828, and the tubing gradient is 0.446. The iteration on netstroke converged in 2 iterations while the interation on damping converged in 4 iterations.
The method of Position calculated 81.45 % pump fillage, while the method of Loads 74.79 and the method of Positions 75.79. The first interval of most likelihood is [76, 79] and the second is [73, 76]. The final pump fillage value is 75.39%.

In Figure 9, results from the MEJ package are applied to field data Example 6. The theoretical fluid load lines read 1188 and -11 lbs, while the calculated fluid load lines read 1188 and -225. The polished rod horsepower is 0.49 while the pump horsepower is 0.36.

The upstroke damping factor is 0.99 while the downstroke damping factor is 0.25. The hydraulic horsepower is 0.7, clearly erroneous from wrong input. This well is severely pumped off. Also the well produces high viscous fluids, this combination can make it difficult to dissociate between a severely pumped off card and one showing a tagging well. The calculated fluid level is 1468, and the tubing gradient is 0.436. The iteration on netstroke converged in 2 iterations while the interation on damping converged in 2 iterations.

The method of Position calculated 4.01 % pump fillage, while the method of Loads 4.01 and the method of Positions 6.49. The first interval of most likelihood is [4, 7] and the second is [97, 100]. The final pump fillage value is 4.83%.
The results in this section show the robustness and accuracy of the MEJ package. The PFC method is the first of its kind in the sense that it combines multi-method approach to tackle the different conditions arising downhole. As mentioned above, different downhole conditions can dramatically alter the shape of a card. This multi-method approach was designed to give an accurate pump fillage value for a wide variety of downhole conditions, when most other pump fillage calculation are just approximations.

4. CONCLUSIONS AND RECOMMENDATIONS

Combining the Modified Everitt-Jennings method with the iteration on dual damping factors, the pump fillage calculation makes a innovative, robust and accurate way of controlling a sucker rod well. The modified Everitt-Jennings method brings a step by step solving of the position and load down the wellbore allowing for stress computation at every node down the wellbore or at any specific depth input by the user for better stress analysis and management. The iteration on damping allows for optimum damping factor selection, which allows for better control of large groups of wells. The pump fillage calculation gives accurate measure for the pump fillage regardless of downhole conditions, which is vital in the control of a sucker rod well.

Even though, the wave equation assumes a vertical-hole model, often it is applied to wells having significant deviation. However, since the Fluid Load Line Calculation has the ability to diagnose the presence of mechanical friction using a concavity test, this is the only model in existence capable of identifying mechanical friction without a deviation survey and controlling the well accordingly. This ensures accurate downhole data regardless of downhole conditions.

The modified Everitt-Jennings method along with the iteration damping and pump fillage calculation can positively affect the production and lengthen the life of any well through better day to day control.

REFERENCES

1. Ehimeakhe, V.: “Calculating Pump Fillage for Well Control using Transfer Point Location”, SPE Eastern Regional Meeting, 12-14 October 2010, Morgantown, West Virginia, USA.
2. Ehimeakhe, V.: “Comparative Study of Downhole Cards Using Modified Everitt-Jennings Method and Gibbs Method”, Southwestern Petroleum Short Course 2010.
3. Everitt, T. A. and Jennings, J. W.: “An Improved Finite-Difference Calculation of Downhole Dynamometer Cards for Sucker-Rod Pumps,” paper SPE 18189 presented at the 63rd Annual Technical Conference and Exhibition, 1988.
4. Gibbs, S. G.: “A Review of Methods for Design and Analysis of Rod Pumping Installations,” SPE 9980 presented at the 1982 SPE International Petroleum Exhibition and Technical Symposium, Beijing, March 18-26.
5. Gibbs, S. G.: “Design and Diagnosis of Deviated Rod-Pumped Wells”, SPE Annual Technical Conference and Exhibition, Oct 6-9, 1991, Dallas, USA.
6. Gibbs, S.G.: “Method of Determining Sucker-Rod Pump Performance,” U.S. Patent No. 3,343,409 (Sept. 26, 1967).
7. Knapp, R. M.: “A Dynamic Investigation of Sucker-Rod Pumping,” MS thesis, U. of Kansas, Topeka (Jan. 1969).
8. Lukasiewicz, S. A.: “Dynamic Behavior of the Sucker Rod String in the Inclined Well”, Production Operations Symposium, April 7-9, 1991, Oklahoma City, Oklahoma, USA.
9. Pons-Ehimeakhe, V.: “Modified Everitt-Jennings Algorithm with Dual Iteration on the Damping Factors.”, 2012 SouthWestern Petroleum Short Course, Lubbock TX, April 17-18th.
10. Pons-Ehimeakhe, V.: “Implementing Coulombs Friction For The Calculation of Downhole Cards in Deviated Wells.”, 2012 SouthWestern Petroleum Short Course, Lubbock TX, April 17-18th.
11. Schafer, D. J. and Jennings, J. W.: “An Investigation of Analytical and Numerical Sucker-Rod Pumping Mathematical Models,” paper SPE 16919 presented at the 1987 SPE Annual Technical Conference and Exhibition, Dallas, Sept. 27-30.
12. Snyder, W. E.: “A Method for Computing Down-Hole Forces and Displacements in Oil Wells Pumped with Sucker Rods,” paper 851-37-K presented at the 1963 Spring Meeting of the API Mid-Continent District Div. of Production, Amarillo, March 27-29.
13. Takács, G.: “Sucker-Rod Pumping Manual.” PennWell, 2002.

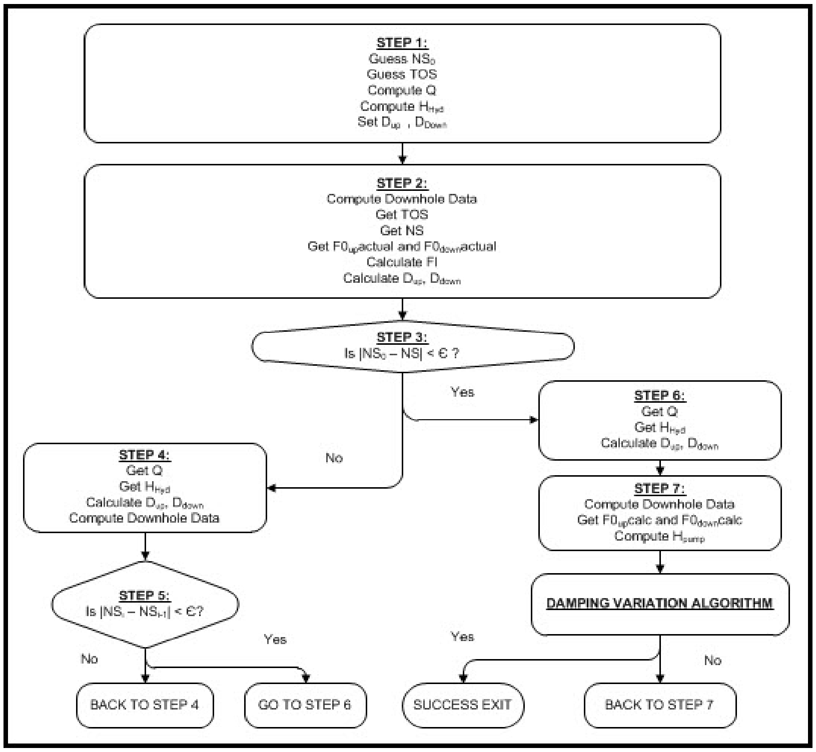

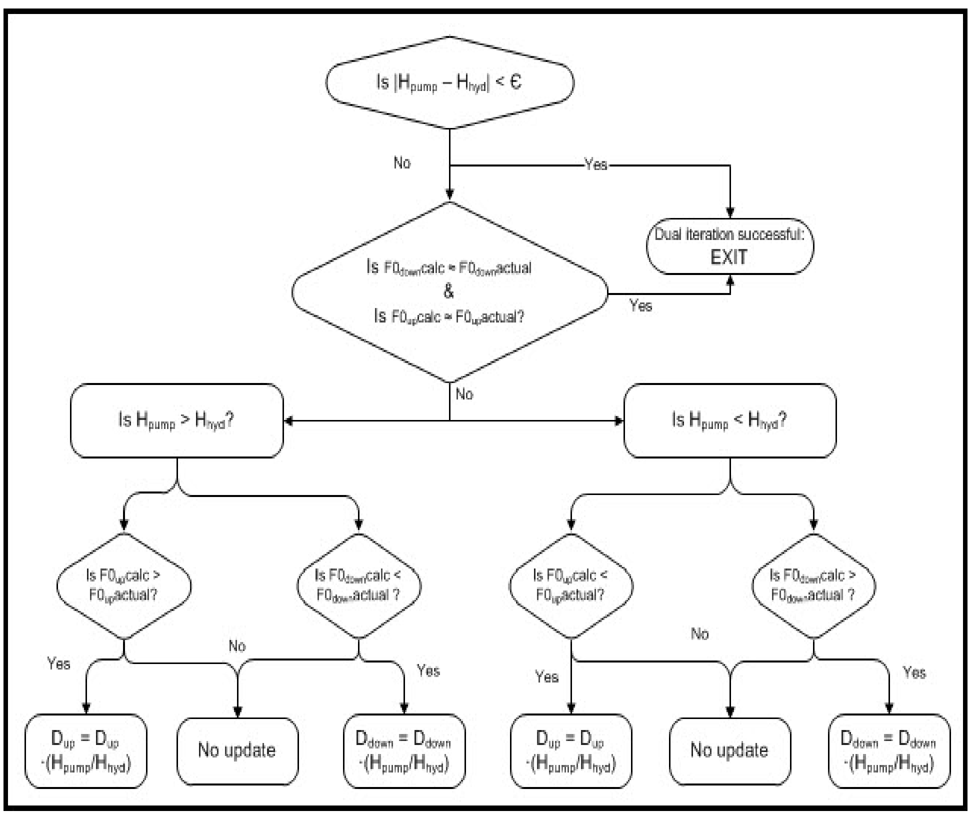

Figure 1, 2: Iteration on dual damping factors flowcharts.

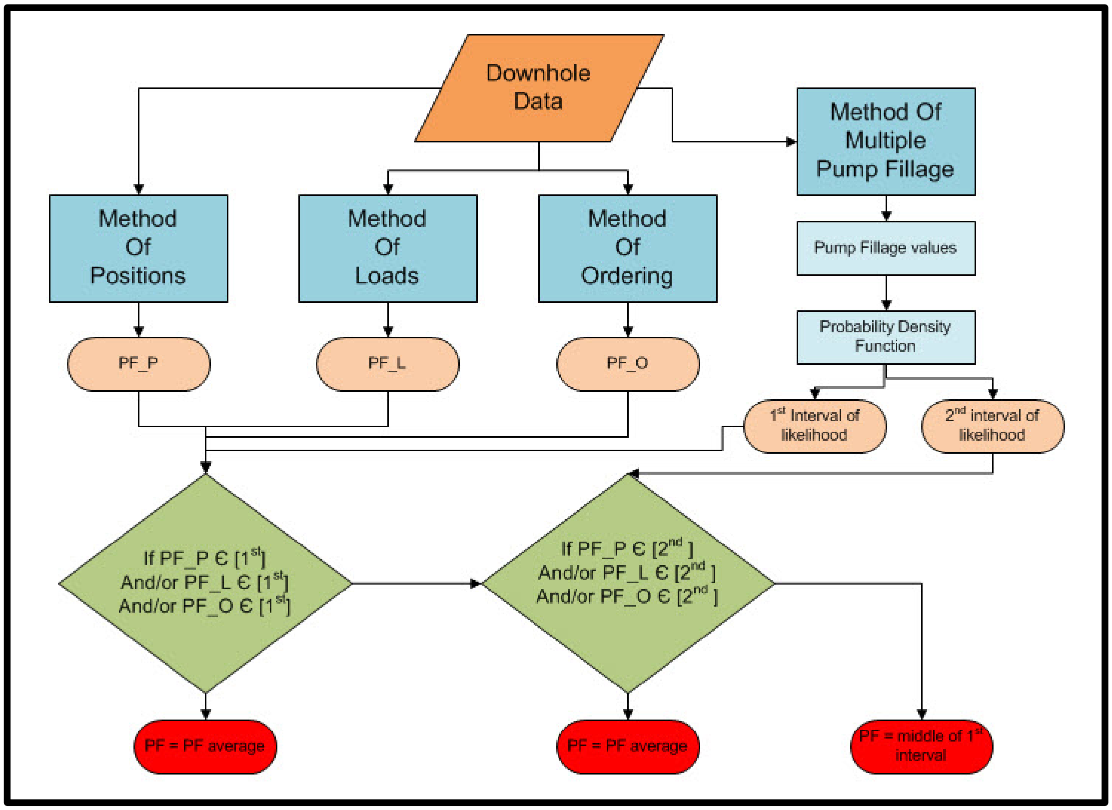

Figure 2: Pump Fillage Calculation (PFC) flowchart.

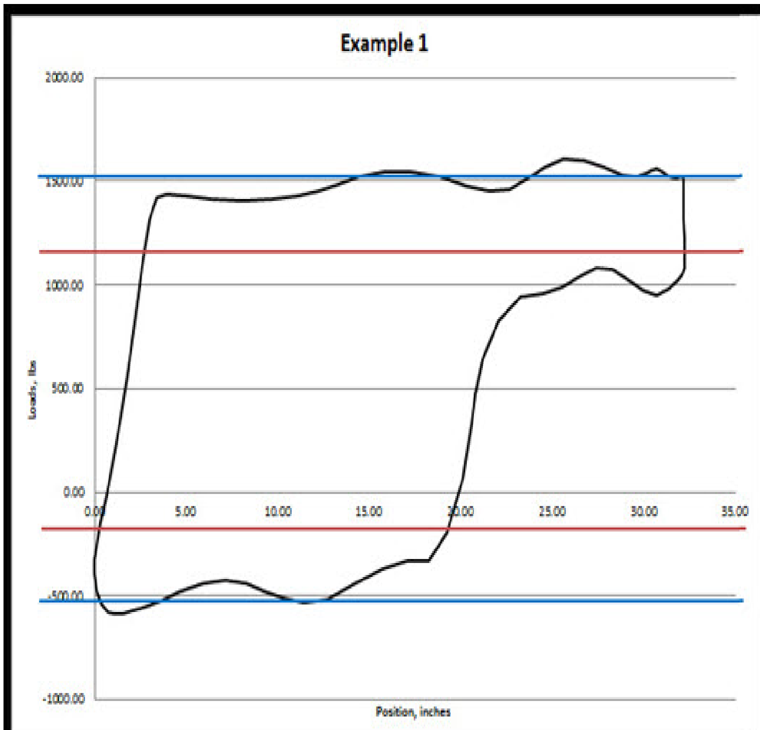

Fluid Load Line Calculation	
F0_up_theo	1219
F0_up_calc	1561
F0_down_theo	-193
F0_down_calc	-546
Tubing Gradient	0.36
Pump Fillage Calculation	
Method of Positions	64.51
Method of Loads	59.82
Method of Orders	64.51
1st interval	[61, 64]
2nd interval	[64, 67]
Final PF	62.94
Iteration on Damping	
Upstroke Damping	0.25
Downstroke Damping	0.5
Polished Rod HP	0.87
Hydraulic HP	1.119
Pump HP	0.76
Fluid level	1160
Number of Iterations	2, 1

Figure 1: Downhole card and results from MEJ package applied to Example 1.

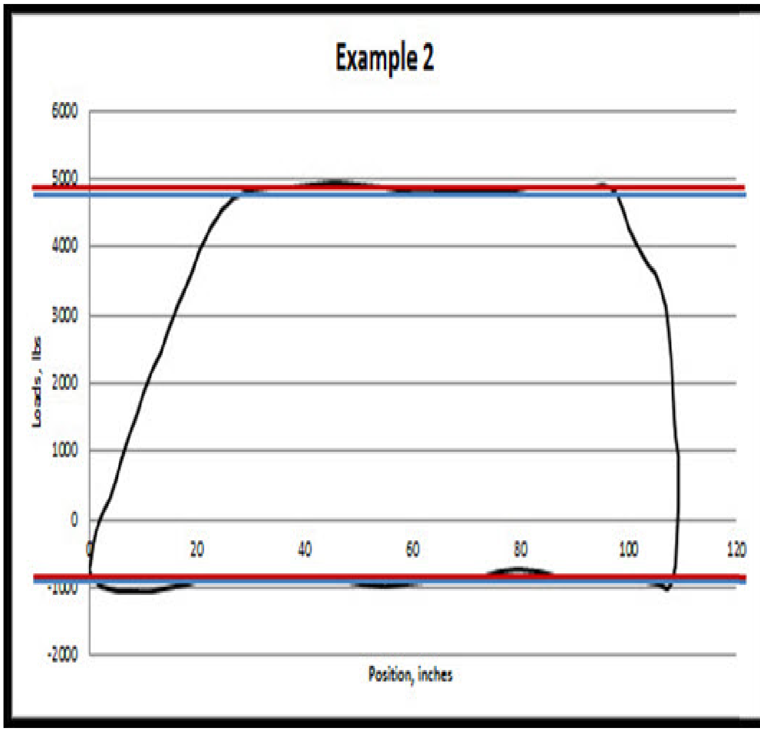

Fluid Load Line Calculation	
F0_up_theo	4876
F0_up_calc	4818
F0_down_theo	-920
F0_down_calc	-931
Tubing Gradient	0.45
Pump Fillage Calculation	
Method of Positions	100.00
Method of Loads	100.00
Method of Orders	100.00
1^{st} interval	[100, 101]
2^{nd} interval	[91, 94]
Final PF	100.00
Iteration on Damping	
Upstroke Damping	0.25
Downstroke Damping	0.5
Polished Rod HP	8.01
Hydraulic HP	5.58
Pump HP	6.84
Fluid level	7285
Number of Iterations	2, 1

Figure 2: Downhole card and results from MEJ package applied to Example 2.

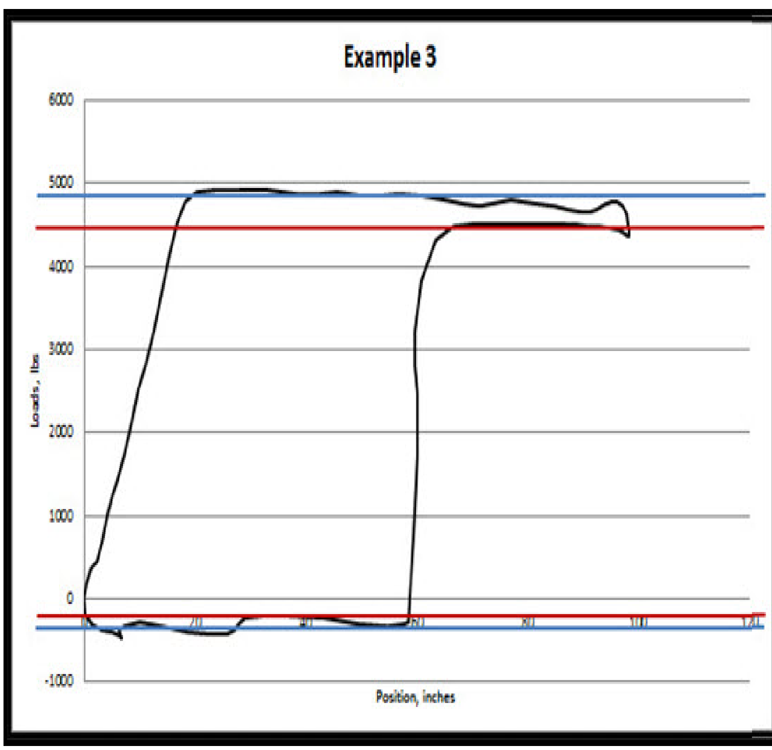

Fluid Load Line Calculation	
F0_up_theo	4415
F0_up_calc	4815
F0_down_theo	-276
F0_down_calc	-354
Tubing Gradient	0.40
Pump Fillage Calculation	
Method of Positions	60.70
Method of Loads	60.35
Method of Orders	61.01
1^{st} interval	[61, 64]
2^{nd} interval	[58, 61]
Final PF	60.69
Iteration on Damping	
Upstroke Damping	0.25
Downstroke Damping	0.5
Polished Rod HP	2.67
Hydraulic HP	3.70
Pump HP	2.28
Fluid level	6558
Number of Iterations	2, 1

Figure 3: Downhole card and results from MEJ package applied to Example 3.

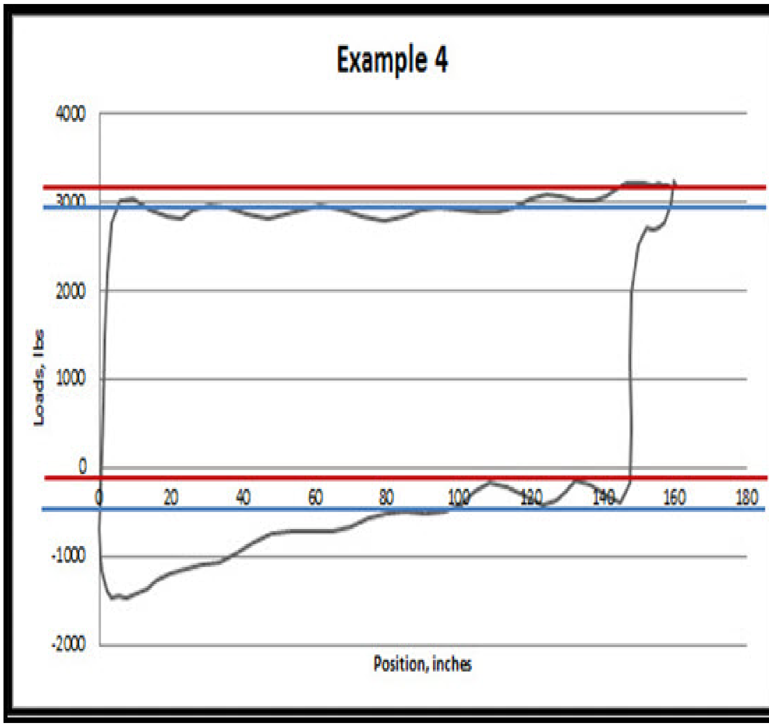

Fluid Load Line Calculation	
F0_up_theo	3172
F0_up_calc	2967
F0_down_theo	-97
F0_down_calc	-241
Tubing Gradient	0.39
Pump Fillage Calculation	
Method of Positions	92.05
Method of Loads	92.05
Method of Orders	92.21
1st interval	[91, 94]
2nd interval	[97, 100]
Final PF	92.10
Iteration on Damping	
Upstroke Damping	0.25
Downstroke Damping	0.99
Polished Rod HP	6.42
Hydraulic HP	3.08
Pump HP	5.29
Fluid level	2787
Number of Iterations	2, 2

Figure 4: Downhole card and results from MEJ package applied to Example 4.

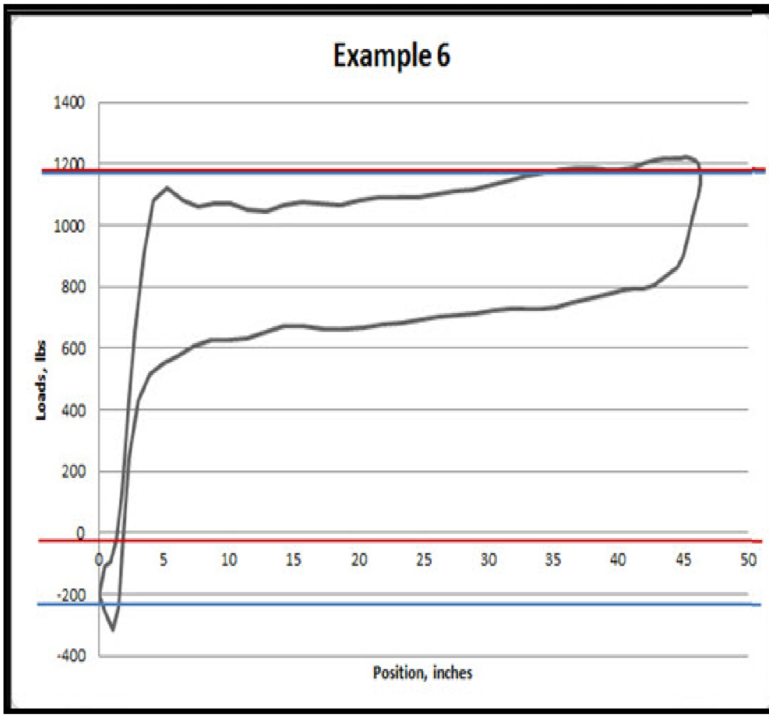

Fluid Load Line Calculation	
F0_up_theo	1188
F0_up_calc	1188
F0_down_theo	-11
F0_down_calc	-225
Tubing Gradient	0.436
Pump Fillage Calculation	
Method of Positions	4.01
Method of Loads	4.01
Method of Orders	6.49
1st interval	[4, 7]
2nd interval	[97, 100]
Final PF	4.83
Iteration on Damping	
Upstroke Damping	0.99
Downstroke Damping	0.50
Polished Rod HP	0.49
Hydraulic HP	0.70
Pump HP	0.36
Fluid level	1468
Number of Iterations	2, 2

Figure 6: Downhole card and results from MEJ package applied to Example 6.